Fluorescence Study on the Swelling Behavior of Comb-Type Grafted Poly(*N*-isopropylacrylamide) Hydrogels

Masahiko Annaka,*,† Chiduru Tanaka,† Takayuki Nakahira,† Masaaki Sugiyama,‡ Takao Aoyagi,§ and Teruo Okano⊥

Department of Materials Technology, Chiba University, 1-33, Yayoi-cho, Inage-ku, Chiba-shi, Chiba 263-8522, Japan; Department of Physics, Kyushu University, 6-10-1, Hakozaki, Higashi-ku, Fukuoka-shi, Fukuoka 812-8581, Japan; Graduate School of Science and Engineering, Kagoshima University, Korimoto, kagoshima-shi, Kagoshima 890-0065, Japan; and Institute of Biomedical Engineering, Tokyo Women's Medical University, 8-1, Kawada-cho, Shinjyuku-ku, Tokyo 162-8666, Japan

Received May 3, 2002; Revised Manuscript Received June 25, 2002

ABSTRACT: The shrinking mechanism of comb-type grafted poly(*N*-isopropylacrylamide) gel due to temperature jump across its volume transition temperature has been investigated. Grafted chains or gel networks were labeled by a dansyl probe, and the temporal change in microenvironment of the dansyl-labeled gel was investigated by means of fluorescence spectroscopy. The comb-type grafted poly(*N*-isopropylacrylamide) gel exhibited a rapid shrinking compared to normal-type NIPA gel, and the change in its microenvironment was found to become hydrophobic more than 10 times faster than normal-type poly(*N*-isopropylacrylamide) gel by observation of temporal change in the maximum emission wavelength, λ_{em}, of the dansyl group. The freely mobile characteristics of grafted chains are expected to show the rapid dehydration to make tightly packed globules with temperature, followed by the subsequent hydrophobic intermolecular aggregation of dehydrated graft chains. The dehydrated grafted chains created the hydrophobic cores, which enhance the hydrophobic aggregation of the networks.

1. Introduction

In recent years, considerable research attention has been focused on hydrogels that are able to alter their volume and properties in response to environmental stimuli such as temperature, pH, and ionic strength.[1−7] Because of their drastic swelling in response to environmental stimuli, these polymeric hydrogels have been investigated for many biomedical and pharmaceutical applications, including controlled drug delivery, molecular separation, tissue culture substrate, and materials for improved biocompatibility.[8−14] Among these "intelligent" gels, temperature- and pH-sensitive hydrogels are most widely investigated. However, since the process is diffusion-controlled, the rate of gel swelling and shrinking is strongly dependent on the size of gel. On the basis of the cooperative diffusion of polymer network in a medium, the Tanaka−Fillmore theory indicates that the characteristic time of gel swelling and shrinking is described by the following equation:[15]

$$\tau \approx R^2/D \qquad (1)$$

where R and D are the size of gel and the cooperative diffusion coefficient of gel network, respectively. For typical polymer gels, D is on the order of $10^{-7}-10^{-6}$ cm^2/s, depending on polymer concentration, cross-linking density, etc. Since it is not easy to increase the value of D by a factor of 10^2 or more, a reduction of gel size has been considered to be the only way to achieve a quick response.

Recent studies, however, have shown that the rate of gel shrinking could be accelerated by (i) introducing a comb-type grafted chain,[7,16,17] (ii) a microporous structure prepared by γ-irradiation,[18] (iii) a phase-separated structure prepared under the existence of diluents,[19] or (iv) having a pathway of water by incorporating hydrophilic chains.[17] With regard to (i), Okano et al. developed a novel architecture of NIPA gel, which exhibited a drastic acceleration of the shrinking rate compared to that of a conventional NIPA gel. Dangling chains in a gel can easily collapse on an external stimulus because one side of the chain is free, which induces a strong shrinking tendency in a gel.

Fluorescence methods, such as steady-state spectroscopy, fluorescence anisotropy, and fluorescence decay measurement, have been shown to be quite effective in the investigation for the microscopic environment around a chromophore.[20−23] A number of studies have been reported on the use of excimer or exciplex formation in polymeric systems to examine local segment mobility, phase separation, and polymer compatibility. The fluorescence depolarization method has been widely used to monitor molecular motion in polymers, molecular aggregates, and biological systems. Although the fluorescence technique was widely used in polymer systems, a few studies have been reported on polymer gels.[24−30] Pyrene and dansyl probes are the most desirable candidates. The pyrene scale for the solvent polarity is well established on the relative intensity I_1/I_3. However, this probe exhibits a strong tendency to form exciplexes in water at relatively low concentration, which limits its application in aqueous media. The dansyl probe has been widely used as a fluorescence probe to study conformational transition in protein and synthetic polymers. This group has a photophysical property that gives information about the local polarity and mobility of the microenvironment as well as the binding behavior of the group.

The first fluorescence probe study on a polymer gel was carried out by Horie et al. to investigate the

† Chiba University.
‡ Kyushu University.
§ Kagoshima University.
⊥ Tokyo Women's Medical University.
* To whom correspondence should be addressed.

10.1021/ma020683y CCC: $22.00 © 2002 American Chemical Society
Published on Web 08/30/2002

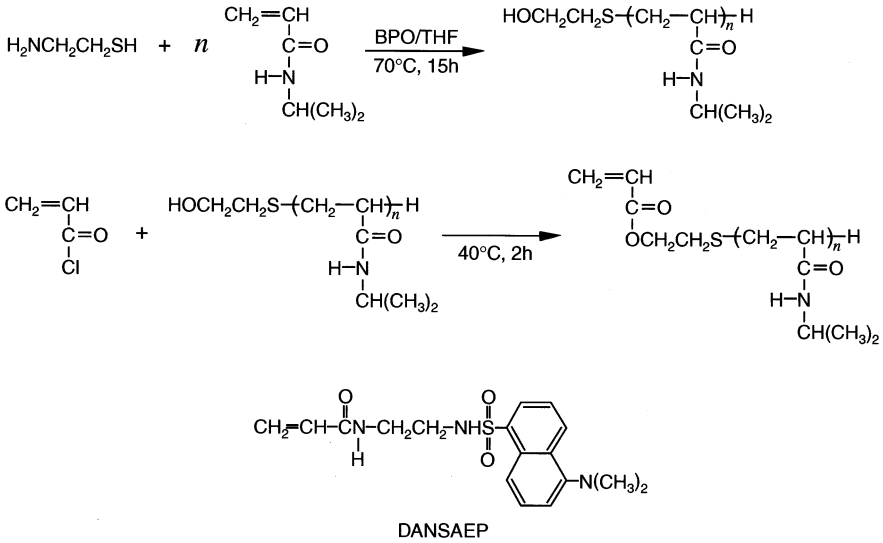

Figure 1. Preparation of *N*-isoprppylacrylamide (NIPA) macromonomer and the chemical structure of dansyl-labeled monomer (DANSAEP).

hydrophobicity and dynamic characteristics of cross-linked polystyrene with dansyl probe.[24] They have successfully applied the fluorescence depolarization technique to investigate the volume phase transition of acrylamide gel network induced by the change in solvent composition and/or pH. They revealed that the volume phase transition of polyacrylamide gels is caused by the change in the solvation of the macromolecular chains, which alters the intra- and intermolecular interactions and chain conformation. The rotational mobility of the probe attached to polymer network becomes infinite at the transition point due to the dynamic fluctuation of the network.[25−30]

The shrinking behavior in NIPA gels has so far been studied by simple swelling ratio measurements as a function of time. Although these studies demonstrated essential roles of the hydrophobic interactions for triggering volume phase transitions in gels, it has not disclosed any microscopic view of the NIPA gel. In this study, therefore, we investigated the temporal change in microenvironment of dansyl-labeled conventional normal-type and comb-type grafted gel by means of fluorescence spectroscopy in order to elucidate the shrinking mechanism of the gels.

2. Experimental Section

2.1. Materials. *N*-Isopropylacrylamide (NIPA; Kohjin Co.) was recrystallized form the mixture of toluene and *n*-hexane. Tetrahydrofuran (THF; Kanto Chemical Co., Ltd.), diethyl ether (Kanto Chemical Co., Ltd.), dansyl chloride (Aldrich), and acryloyl chloride (Aldrich) were purified just before use according to standard procedures. 2-Hydroxyethanethiol (HESH; Tokyo Kasei Kogyo Co., Ltd.), benzoyl peroxide (BPO; Nakarai Tesque Co.), *N*,*N*′-methylenebis(acrylamide) (BIS; Kanto Chemical Co.), *N*,*N*′-tetramethylethylenediamine (TEMED; Kanto Chemical Co.), and ammonium peroxide (APS; Kanto Chemical Co.) were used as received.

2.2. Preparation of Dansyl-Labeled Monomer. *N*-[2-[[[5-(*N*,*N*-dimethylamino)-1-naphthalenyl]sulfonyl]amino]ethyl]-2-propenamide (DANSAEP, Figure 1) was prepared by the method as described previously.[30]

2.3. Macromonomer Synthesis. A semitelechelic PNIPA with a terminal hydroxyl end group (semi-telechelic PNIPA−OH) was prepared by radical telomerization of NIPA monomer using HESH as a chain transfer agent. NIPA macromonomer was synthesized by the esterification of acryloyl chloride with semi-telechelic PNIPA−OH. Dansyl-labeled NIPA macromonoer was prepared in a same manner to the preparation of the corresponding nonlabeled NIPA macromonomer except for addition of DANSAEP (Figure 1).

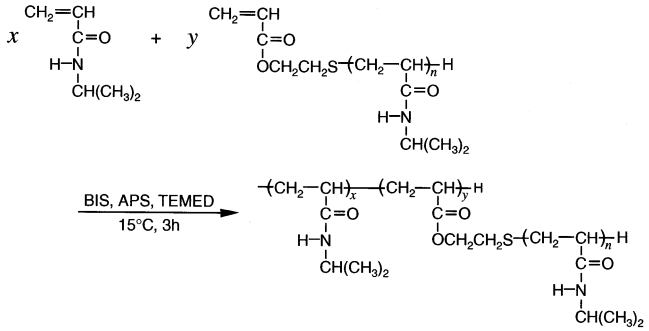

Figure 2. Preparation of the comb-type grafted NIPA gel.

2.4. Preparation of Poly(*N*-isopropylacrylamide) Hydrogels. Comb-type grafted and normal-type poly(*N*-isopropylacrylamide) hydrogels were prepared by radical polymerization (Figure 2).

2.5. Swelling Experiments. A gel was placed in a glass cell, the temperature of which was controlled to within 0.1 °C of the desired temperature. The swelling degree of gel, d/d_0, was obtained by measuring the diameter of the cylindrical gel, d, under a microscope.

2.6. Shrinking Kinetics of Gels. The gel sample was placed in a thermostated cell filled with distilled deionized water, the temperature of which was controlled to within 0.1 °C of the desired temperature. The temperature-jump (T-jump) experiments were carried out by exchanging the circulating water which temperatures were set to desired temperatures. The time required for temperature jump was about 30 s. The measurement was repeated at least three times, and its average was used as the value of d.

2.7. Gel Permeation Chromatography. The molecular weight of semi-telechelic PNIPA−OH was estimated by gel permeation chromatography, using TSKgel GMPW$_{HR}$ column and a TOSOH RI-8022 detector. HPLC grade DMF with 10 mM LiCl was used as the mobile phase at a flow rate 1 mL/min. Calibration was carried out with monodisperse poly(ethylene glycol) standards purchased from TOSOH Corp.

2.8. NMR Spectroscopy. ^{1}H NMR spectra were recorded on a JEOL LA-400 spectrometer in $CDCl_3$ with TMS as the internal reference.

2.9. Measurements of Photophysical Properties. The fluorescence emission spectra were recorded on a Hitachi F-4010 fluorescence spectrophotometer with a thermostated cell filled with distilled deionized water, the temperature of

Table 1. Feed Composition for Preparation of NIPA Normal-Type Gel (NG) and Comb-Type Grafted NIPA Gel (GG)

sample code	NG	GG15g	GG15m	GG30g	GG30m
macromonomer (wt %)	0	15	15	30	30
NIPA monomer (g)	15.60	10.92	10.92	10.92	10.92
macromonomer (g)			2.34		4.68
DANSAEP (g)	0.043		0.043		0.043
dansyl-labeled macromonomer (g)		2.34		4.68	
BIS (g)	0.266	0.266	0.266	0.266	0.266
TEMED (μL)	48	48	48	48	48
APS (g)	0.008	0.008	0.008	0.008	0.008
DMF/water (20/80 in vol) (mL)	100	100	100	100	100

Table 2. Preparation and Characterization of NIPA Macromonomer and Dansyl-Labeled NIPA Macromonomer

	NIPA (g)	DANSAEP (g)	HESH (g)	BPO (g)	THF (mL)	conv (%)	M_n	M_w	M_n/M_w
NIPA macromonomer	33.9		0.469	0.121	100	70.0	5170	7340	1.42
dansyl-labeled NIPA macromonomer	33.9	0.136	0.469	0.121	100	70.4	5070	7125	1.41

which was controlled to within 0.1 °C of the desired temperature. The excitation wavelength was set at 345 nm. The measurement of the temporal shift in λ_{em} was carried out within the wavelength range of λ_{em} of the initial temperature and that of destination temperature. The scanning rate was set to 10 nm/s, and the period for scanning the whole range was about 25 s. The measurement was repeated at least three times, and its average was used as the value of λ_{em}. The fluorescence anisotropy ratio, *r*, was calculated from four polarized fluorescence spectra by using

$$r = (I_{VV} - GI_{VH})/(I_{VV} + 2GI_{VH}) \qquad G = I_{HV}/I_{HH} \qquad (2)$$

where *I* is the fluorescence intensity and the subscripts represent the orientation of polarizers (V is vertical and H is horizontal), which are located for incident light (the first subscript) and for emitted light (the second subscript). The *G* value was used for the correcting the depolarization characteristics of the grating-type monochromator. The anisotropy, *r*, were averaged for emission from 400 to 650 nm.

3. Results and Discussion

3.1. Preparation of NIPA Macromonomer. NIPA macromonomer and dansyl-labeled NIPA macromonomer were prepared by radical telomerization of NIPA monomer using HESH as a chain transfer agent (Figure 1). To confirm the polymerization of a semi-telechelic PNIPA−OH, ^{1}H NMR spectroscopy measurements were carried out. In ^{1}H NMR spectroscopy measurements, the spectrum of semi-telechelic PNIPA−OH exhibited peaks at 1.1 ppm (−CH_3) and 4.0 ppm (−CH−), while the peak at 2.7 ppm was due to a chain transfer agent (HESH). Two broad peaks at 1.6 and 2.2 ppm due to methylene proton and methyne proton were observed, while the peaks of vinyl proton at 5.8−6.2 ppm were not detected.

The number-average molecular weights of both NIPA macromonomer and dansyl-labeled NIPA macromonomer were determined to be 5000 by gel permeation chromatography. The feed composition and characteristics of NIPA mocromonomers are listed in Table 1.

3.2. Preparation of NIPA Hydrogels. Comb-type grafted NIPA gels were prepared by radical polymerization of NIPA monomer and NIPA macromonomer in the presence of BIS as a cross-linker in DMF/water mixture (20/80 in volume) at 5 °C for 24 h in capillaries of inner diameter 1.0 mm (=d_0) (Figure 2). Dansyl-labeled NIPA hydrogel was prepared in the same manner as the preparation of the corresponding nonlabeled NIPA hydrogel macromonomer, except for addition of DANSAEP or dansyl-labeled NIPA macromonomer. The feed compositions of monomers and other chemicals are listed in Table 2. The total amount of NIPA monomer unit (NIPA monomer + NIPA macromonomer) was kept constant, and the weight ratio of NIPA macromonomer to NIPA monomer was chosen to be 15% (w/w) and 30% (w/w), which are designated GG15 and GG30, respectively. Normal-type NIPA gel was also prepared without adding NIPA macromonomer, which is designated NG. The characters "m" and "g" of the sample name show the position labeled by dansyl probe: "m" and "g" respectively indicate the polymer networks and grafted chains are labeled by the dansyl probe (Table 2). The weight conversions of graft-type gels and normal-type gel from monomers are 85% and 90%, respectively. The feed compositions are listed in Table 2.

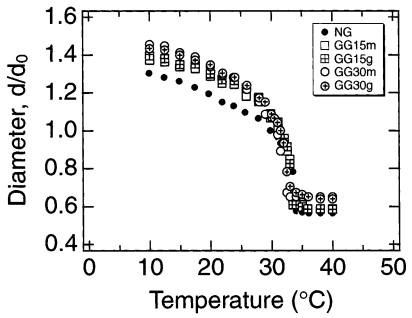

Figure 3. Equilibrium swelling degrees, d/d_0, of graft-type gel and normal-type gel are plotted as a function of temperature.

3.3. Equilibrium Swelling Degree. Equilibrium swelling degrees, d/d_0, of graft-type and normal-type gels are plotted as a function of temperature in Figure 3. The phase behaviors indicate that the graft-type gels show the same transition temperature (34 °C) as that of normal-type gel. Below the transition temperature, graft-type gels exhibit a higher swelling ratio than the normal-type gel. The GG30 gel showed a slightly higher swelling ratio than the GG15 gel. As the grafted chains are structurally separated from the backbone cross-linked network, stronger hydration may be possible. This chain expansion may result in increased hydration in graft-type gel. Controlling the amount of grafted chain can regulate the equilibrium swelling properties of hydrogels.

3.4. Steady-State Photophysical Properties of Dansyl Groups Attached to the Gels. The fluorescence spectroscopy of dansyl derivatives has been studied extensively. It is relatively insensitive to quenching by oxygen and trace impurities. The absorption maximum is essentially independent of the medium.[21−23,31]

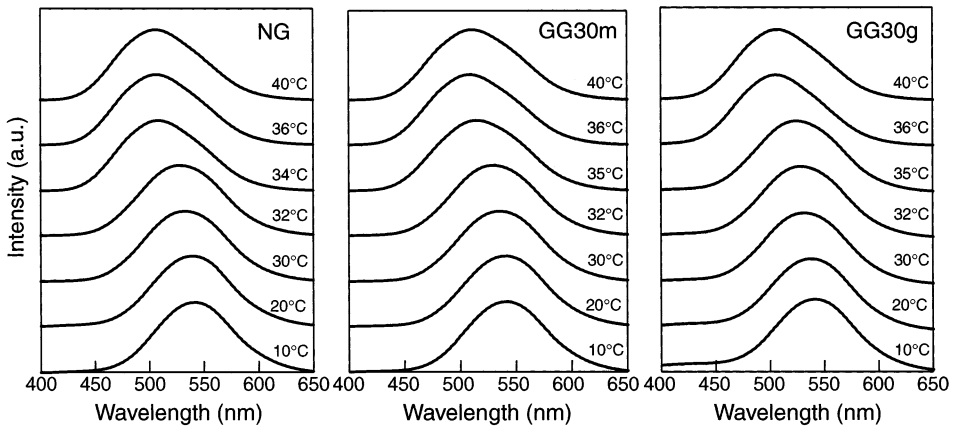

Figure 4. Fluorescence spectra of the dansyl probe attached to the network of NG, GG30g, and GG30m gels at selected temperatures.

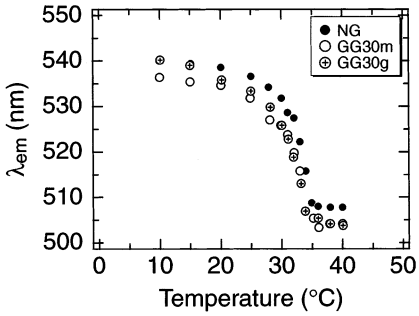

Figure 5. Wavelength of maximum emission, λ_{em}, of dansyl probe attached to NG, GG30m, and GG30 g as a function of temperature.

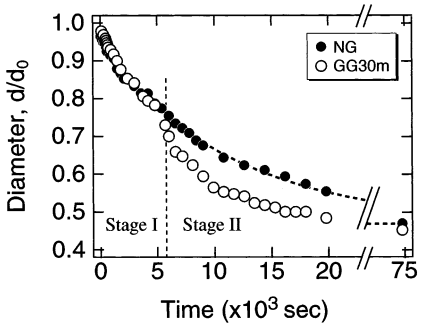

Figure 6. Variation of the degrees of swelling, d/d_0 ($\equiv d(t)/d_0$), of the NG and GG30m after T-jump from 10 to 35 °C. The inset is the semilogarithmic plot of the same data. The lines are the fit with eq 2.

Figure 4 shows the fluorescence spectra of the dansyl probe attached to the network of NG, GG30g, and GG30m gels at various temperatures. The dansyl group is known to be sensitive to local hydrophobicity, polarity, and mobility. When the dimethylamino group takes a coplanar conformation with a naphthyl group in the nonpolar or the hydrophobic microenvironment, the maximum emission wavelength, λ_{em}, of the dansyl group is about 430 nm, and when the dimethylamino group takes a twisted intermolecular charge transfer (TICT) state with a naphthyl group in the polar or the hydrophilic microenvironment, λ_{em} is about 580 nm.[21,32] The shift of λ_{em} from 430 to 580 nm is determined by the twisting angle and speed of the dimethylamino group with the naphthyl group, which is induced by local hydrophobic interaction, polarity, viscosity, and free volume.[25,26,31−38] For these NIPA gels, the shift of λ_{em} provides information on the local microenvironment of dansyl probes in different domains. Figure 5 indicates the wavelength of maximum emission as a function of temperature. The dansyl probe in each system undergoes a blue shift in the maximum emission wavelength at the transition from swollen to collapsed state, indicating that the probe experiences a more hydrophobic microenvironment. The transition of the λ_{em} occurs in the following order: GG30g ≈ GG30m < NG. The graft NIPA gels having freely mobile ends are sufficiently hydrated and contain a large amount of free water.[7,16] Therefore, the graft NIPA gels are readily dehydrated with temperature.

It is worthy to note that the GG30m gel exhibits the rapid change in λ_{em} at lower temperature than that of NG. Both NG and GG30m gel networks are labeled by a dansyl probe. The observed difference in shift of λ_{em} may be ascribed to the freely mobile characteristics of NIPA graft chains, which are expected to show a rapid dehydration to make tightly packed globules with temperature, followed by the subsequent hydrophobic intermolecular aggregation of dehydrated graft chains. The dehydrated graft NIPA chains created the hydrophobic cores, which enhance the hydrophobic aggregation of the NIPA networks.

3.5. Kinetics of Shrinking/Swelling Process. The kinetics of swelling of gel was treated by Tanaka and Fillmore.[15] The time variation of gel size, e.g., the gel diameter, could be described by a single-exponential function

$$\frac{d(t)-d(\infty)}{d(0)-d(\infty)}=\frac{d(t)/d_0-d(\infty)/d_0}{d(0)/d_0-d(\infty)/d_0}\approx\frac{6}{\pi^2}\exp\left(-\frac{t}{\tau}\right) \quad (3)$$

where $d(t)$ is the gel diameter at time t and τ is the characteristic time for swelling. It has been confirmed that eq 3 was also valid for the shrinking kinetics as far as the shrinking did not accompany phase separation.[39,40] However, the shrinking kinetics is completely different from that predicted by Tanaka and Fillmore when the size of gel changes drastically or a phase separation is accompanied. This is due to the fact that the theory is limited to the linear regime and the collective diffusion constant is assumed to be invariant upon shrinking/swelling.[15]

Figure 6 shows the variation of the degrees of swelling, d/d_0 ($\equiv d(t)/d_0$), of the gels after T-jump from 10 to

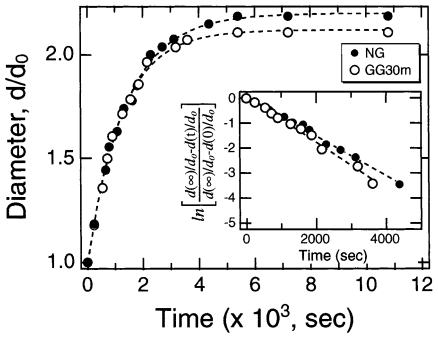

Figure 7. Changes in the degrees of swelling, d/d_0 ($\equiv d(t)/d_0$), of NG and GG30m during the swelling process by T-jump from 35 to 10 °C.

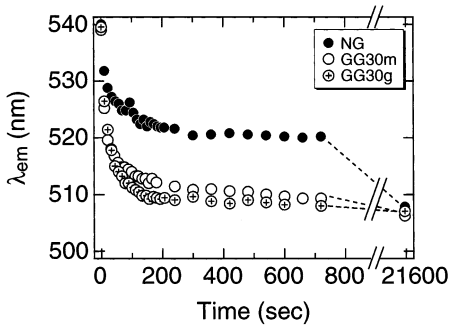

Figure 8. Temporal changes in the maximum emission wavelength, λ_{em}, of dansyl probe for the NG, GG30m, and GG30 g after T-jump from 10 to 35 °C.

Table 3. Values of the Time Required for Half-Shrinking, $t_{1/2}$, for Gels T-Jumped from 10 to 35 °C

sample code	$t_{1/2}$ (s)	sample code	$t_{1/2}$ (s)
NG	6988	GG30m	3880
GG15m	6457	GG30g	3809
GG15g	6300		

Table 4. Values of the Time Required for Half-Shift, $t_{1/2}$, of λ_{em} for Gels T-Jumped from 10 to 35 °C

sample code	$t_{1/2}$ (s)
NG	150
GG30m	14.3
GG30g	11.9

35 °C. In the case of NG, the change in the swelling ratio is satisfactorily reproduced by eq 3, which indicates that the shrinking process is the diffusion-controlled one with the collective diffusion constant 2.7×10^{-7} cm^2/s. In the case of GG30m, however, the shrinking process is characterized by two stages. In stage I, the process seems to be diffusion-controlled, and a diffusion constant of the gel network is 2.6×10^{-7} cm^2/s. In stage II, however, the shrinking rate is more accelerated than that of stage I. Since analysis with a single-exponential function (eq 3) became no more applicable to whole shrinking process, the time required for half-shrinking, $t_{1/2}$, was defined as follows:[39,40]

$$\frac{d(t_{1/2}) - d(\infty)}{d(0) - d(\infty)} = \frac{d(t_{1/2})/d_0 - d(\infty)/d_0}{d(0)/d_0 - d(\infty)/d_0} = \frac{1}{2} \qquad (4)$$

The values of the time required for half-shrinking, $t_{1/2}$, for gels T-jumped from 10 to 35 °C are summarized in Table 3. $t_{1/2}$ for GG30s' is approximately one-half of that for NG. The NG became opaque immediately after the T-jump from 10 to 35 °C, suggesting that a heterogeneous structure was formed in the gel networks. Since a dense, collapsed polymer layer impermeable to water is formed near the gel surface, the shrinking rate of NG is limited by suppressed water permeation from the gel interior through the collapsed polymer skin. In contrast to NG, introducing 30% (w/w) of NIPA macromonomer (GG30m and GG30g) made the gels shrink faster. Above the transition temperature, grafted chains are dehydrated, and then a hydrophobic aggregation force forms between dehydrated grafted chains. In stage II, therefore, these aggregations of the NIPA chins contribute to an increase in void volume, which allow gel having a pathway of water molecules through the gel by phase separation.

Figure 7 shows the changes in d/d_0 of NG and GG30m during the swelling process by T-jump from 35 to 10 °C. Contrary to the shrinking process, the swelling process is described with a single-exponential function and could be fitted with eq 3. The evaluated values of D for NG and GG30m were 2.4×10^{-7} and 2.2×10^{-7} cm^2/s, respectively. Although no bubbles are formed, a characteristic pattern appears on the surface. The characteristic size of the pattern grows with time at the beginning, followed by a uniform swelling. Therefore, it is clear that swelling kinetics is quite different from the shrinking kinetics. A similar phenomenon was observed by Sato-Matsuo and Tanaka[41] and was explained as buckling of the surface due to swelling at the surface with the inner part remaining in the collapsed state.[41,42]

3.6. Temporal Changes in λ_{em} for T-Jump Process. The temporal changes in microenvironment of dansyl-labeled NG and GG30s' gel were investigated by means of fluorescence spectroscopy. Figure 8 shows the temporal changes in λ_{em} for gels after T-jump from 10 to 35 °C. The observed time-variation behavior of λ_{em} is similar to that of gel size, and analysis with a single-exponential function is not applicable. We defined the time required for half-shift, $t_{1/2}$, of λ_{em} as follows:

$$\frac{\lambda_{em}(t_{1/2}) - \lambda_{em}(\infty)}{\lambda_{em}(0) - \lambda_{em}(\infty)} = \frac{1}{2} \qquad (5)$$

The values of the time required for half-shift, $t_{1/2}$, for gels T-jumped from 10 to 35 °C are summarized in Table 4. The changes in the microenvironment for GG30s' are accelerated by an order of magnitude compared with that for NG. The grafted chains maintain their mobility, while NIPA networks are anchored at several points by cross-linking on each chain restricting the mobility.

The λ_{em} of the dansyl probe decreases initially vary rapidly with time while the diameter of the gel changes only slightly. The dansyl probe is expected to act as a molecular probe sensing the microscopic environment. The position, shape, and intensity of the emission are sensitive to molecular mobility, solvation, and polarity of the microscopic environment around the chromospheres. The temporal change in the diameter and λ_{em} is related to the several factors: variation of dehydration of chains, local viscosity, structural relaxation, and so forth. To understand the microscopic factors that occur during the gel shrinkage, we carried out the fluorescence anisotropy measurements. Figure 9 shows the temporal changes in anisotropy, r, for gels after T-jump from 10

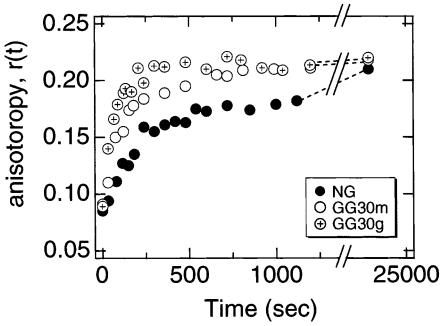

Figure 9. Temporal changes in the anisotropy, *r*, of dansyl probe for the NG, GG30m, and GG30g after T-jump from 10 to 35 °C.

Table 5. Values of the Time Required for Half-Change, $t_{1/2}$, of *r* for Gels T-Jumped from 10 to 35 °C

sample code	$t_{1/2}$ (s)
NG	240
GG30m	108
GG30g	41.3

to 35 °C. The observed time variation behavior of *r* is similar to that of λ_{em}. We defined the time required for half-change, $t_{1/2}$, of *r* as follows:

$$\frac{r(t_{1/2}) - r(\infty)}{r(0) - r(\infty)} = \frac{1}{2} \tag{6}$$

The values of the time required for half-change, $t_{1/2}$, for gels T-jumped from 10 to 35 °C are summarized in Table 5. The values of the time required for half-change in the microviscosity show following order: GG30g < GG30m < NG. As shown in Tables 4 and 5, GG30m and GG30g exhibit a smaller $t_{1/2}$ value for λ_{em} than that for *r*. These observations suggest that the rapid thermal response of the comb-type grafted NIPA gels microscopically attributes to the following mechanism: the rapid dehydration of the freely mobile NIPA graft chains due to the increase in hydrophobicity, and the subsequent hydrophobic intermolecular aggregation of dehydrated graft chains enhances the hydrophobic aggregation of the NIPA networks because of the increase in microviscosity. In the case of NG, however, the temporal change in *r* for NG almost coincides with that in λ_{em}. This is due to the fact that the shrinking of NG is controlled by the collective diffusion of network; therefore, dansyl locally probes both viscosity and hydrophobicity.

The limiting value of *r* in the medium where no rotational diffusion takes place or the Brownian motion is frozen was determined to be 0.325 by extrapolation of *r* to infinite viscosity for the probe monomer with the dansyl group, dansyl-labeled monomer (DANSAEP), in the water/glycerol mixture by Hu et al.[25] It is worth noting that the anisotropy ratio, *r*, shown in Figure 9 does not reach its limiting value, which indicates that the probe constrained in a collapsed gel experiences a high effective viscosity; it still undergoes some rotational motion.

It should be mentioned that the characteristic time, $t_{1/2}$, values of λ_{em} and *r* are much smaller than that of diameter change, which are by a factor of 10 for NG and by a factor of 100 for GGs. The microscopic change is complete faster than macroscopic one. This is likely related to the structural relaxation of gel network and the change in the microscopic structure of gels during the shrinking process, though we cannot give a clear interpretation here. SAXS and SANS may provide powerful tools for studying these phenomena at the molecular level. We are investigating to elucidate the temporal change in microscopic structure of NG and GGs after a T-jump from 10 to 35 °C using SAXS and SANS. A further investigation of the correlation between macroscopic swelling behavior and microscopic structure will be reported in a future publication.

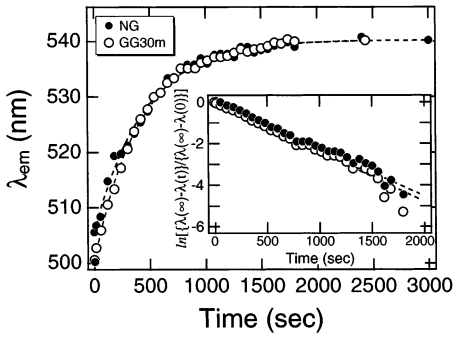

Figure 10. Variation of the maximum emission wavelength, λ_{em}, of dansyl probe for the NG and GG30m during the swelling process by T-jump from 35 to 10 °C. The inset is the semilogarithmic plot of the same data. The lines are the fit with eq 2.

Figure 10 shows the temporal changes in λ_{em} for NG and GG30m during the swelling process by T-jump from 35 to 10 °C. Contrary to the shrinking process, the shift in λ_{em} for NG and GG30m is described with a single-exponential function and could be fitted with eq 2. The evaluated relaxation times for NG and GG30m were 1210 and 1320 s, respectively. These results are consistent with the results obtained from temporal change in gel diameters and indicate that the swelling process is in the linear regime and the collective diffusion constant is assumed to be invariant upon swelling.

4. Conclusion

The shrinking mechanism of comb-type grafted NIPA gel due to temperature jump across its volume transition temperature has been investigated. Grafted chains or gel networks were labeled by a densyl probe, and the temporal change in microenvironment of dansyl-labeled gel was investigated using fluorescence spectroscopy. The change in microenvironment of the comb-type NIPA gel due to T-jump was found to become hydrophobic more than 10 times faster than normal-type NIPA gel by observing the change in the maximum emission wavelength, λ_{em}, of the dansyl group as a function of time. The temporal change in anisotropy indicates the freely mobile characteristics of grafted chains, which expected to show the rapid dehydration to make tightly packed globules with temperature, followed by the subsequent hydrophobic intermolecular aggregation of dehydrated graft chains. The dehydrated grafted chains created the hydrophobic cores, which enhance the hydrophobic aggregation of the networks.

References and Notes

(1) Tanaka, T. *Phys. Rev. Lett.* **1978**, *40*, 820.
(2) Tanaka, T.; Fillmore, D. J.; Sun, S. T.; Nishio, I.; Swislow, G.; Shah, A. *Phys. Rev. Lett.* **1980**, *45*, 1636.
(3) Hirokawa, Y.; Tanaka, T. *J. Chem. Phys.* **1984**, *81*, 6379.
(4) Shibayama, M.; Tanaka, T. *Adv. Polym. Sci.* **1993**, *109*, 1.
(5) Kiler, J.; Scranton, A. B.; Peppas, N. A. *Macromolecules* **1990**, *23*, 4944.
(6) Sukuki, A.; Tanaka, T. *Nature (London)* **1990**, *346*, 345.

(7) Yoshida, R.; Uchida, K.; Kaneko, Y.; Sakai, K.; Kikuchi, A.; Sakurai, Y.; Okano, T. *Nature (London)* **1995**, *374*, 240.
(8) Okano, T., Ed. *Biorelated Polymers and Gels: Controlled Release and Applications in Biomedical Engineering*; Academic Press: New York, 2000.
(9) Okano, T.; Yui, N.; Yokoyama, M.; Yoshida, R. *Advances in Polymeric Systems for Drug Delivery*; Gordon & Breach Science Publishers: Yverdon, Switzerland, 1994; p 67.
(10) Dusek, K., Ed. *Responsive Gels*: *Volume Phase Transition II*; Springer-Verlag: Berlin, 1993.
(11) Hoffman, A. S. *J. Controlled Release* **1987**, *6*, 297.
(12) Hoffman, A. S.; Afrassiabi, A.; Dong, L. C. *J. Controlled Release* **1986**, *4*, 213.
(13) Peppas, N. A.; Korsmeyer, R. W. In *Hydrogels in Medicine and Pharmacy*; Peppas, N. A., Ed.; CRC Press: Boca Raton, FL, 1987; Vol. III, p 122.
(14) Yoshida, R.; Kaneko, Y.; Sakai, K.; Okano, T.; Sakurai, Y.; Bae, Y. H.; Kim, S. W. *J. Controlled Release* **1994**, *32*, 97.
(15) Tanaka, T.; Fillmore, D. *J. Chem. Phys.* **1979**, *70*, 1214.
(16) Kaneko, Y.; Sakai, K.; Kikuchi, A.; Yoshida, R.; Sakurai, Y.; Okano, T. *Macromolecules* **1995**, *28*, 7717.
(17) Kaneko, Y.; Nakamura, S.; Sakai, K.; Kikuchi, A.; Aoyagi, T.; Sakurai, Y.; Okano, T. *Polym. Gels Networks* **1998**, *6*, 333.
(18) Kishi, R.; Hirasa, O.; Ichijo, H. *Polym. Gels Networks* **1997**, *5*, 145.
(19) Wu, X. S.; Hoffman, A. S.; Yager, P. J. *Polym. Sci., Polym. Chem. Ed.* **1992**, *30*, 2121.
(20) Parreno, J.; Pierola, I. F. *Polymer* **1990**, *23*, 4497.
(21) Weber, G. *Biochem. J.* **1952**, *51*, 155.
(22) Strauss, U. P.; Vesnaver, G. *J. Phys. Chem.* **1975**, *79*, 1558.
(23) Shea, K. J.; Stoddard, G. J.; Shavelle, D. M.; Wakui, F.; Choate, R. M. *Macromolecules* **1990**, *23*, 4497.
(24) Horie, K.; Mita, I.; Kawabata, J.; Nakahama, S.; Hirao, A.; Yamazaki, N. *Polym. J.* **1980**, *12*, 319.
(25) Hu, Y.; Horie, K.; Usikim, H. *Macromoecules* **1992**, *25*, 6040.
(26) Hu, Y.; Horie, K.; Usiki, H.; Tsunomori, F.; Yamashita, T. *Macromolecules* **1992**, *25*, 7324.
(27) Hu, Y.; Horie, K.; Torii, T.; Ushiki, H.; Tang, X. *Polym. J.* **1993**, *25*, 123.
(28) Hu, Y.; Horie, K.; Usiki, H.; Tsunomori, F.; Yamashita, T. *Macromolecules* **1993**, *26*, 1761.
(29) Hu, Y.; Horie, K.; Usiki, H. *Polym. J.* **1993**, *25*, 651.
(30) Annaka, M.; Noda, H.; Motokawa, R.; Nakahira, T. *Polymer* **2001**, *42*, 9887.
(31) Ren, B.; Gao, F.; Tong, Z.; Yan, Y. *Chem. Phys. Lett.* **1999**, *307*, 55.
(32) Li, Y. H.; Chan, L. M.; Tyer, L.; Moody, R. T.; Himel, C. M.; Hercules, D. M. *J. Am. Chem. Soc.* **1975**, *97*, 3118.
(33) Hayashi, R.; Tazuke, S.; Frank, C. W. *Macromolecules* **1987**, *20*, 983.
(34) Tazuke, S.; Guo, R. K.; Hayashi, R. *Macromolecules* **1988**, *21*, 1046.
(35) Rotkiewicz, K.; Grellmann, K. H.; Grabowski, Z. R. *Chem. Phys. Lett.* **1973**, *19*, 315.
(36) Grabowski, Z.; Rotkiewicz, K.; Siemiarczuk, A.; Cowley, D. J.; Baumann, W. *Nouv. J. Chim.* **1979**, *3*, 443.
(37) Nakashima, N.; Mataga, N. *Bull. Chem. Soc. Jpn.* **1973**, *46*, 3016.
(38) Bednar, B.; Trnena, J.; Svoboda, P. *Macromolecules* **1991**, *24*, 2054.
(39) Hirose, H.; Shibayama, M. *Macromolecules* **1998**, *31*, 5336.
(40) Shibayama, M.; Nagai, K. *Macromolecules* **1999**, *32*, 7461.
(41) Sato-Matsuo, E.; Tanaka, T. *J. Chem. Phys.* **1988**, *89*, 1695.
(42) Tanaka, T.; Sun, S. T.; Hirokawa, Y.; Katayama, S.; Jucera, J.; Hirose, Y.; Amiya, T. *Nature (London)* **1987**, *325*, 796.

MA020683Y